

Digital Photography, a Tool for Lighting Research: High-resolution sampling of spherical luminance maps with digital photographic technologies applied to diffuseness descriptors

MIGUEL SANTA CLARA¹

¹Department of Architecture, University of Cambridge, Cambridge, UK

ABSTRACT: The ability to accurately measure and represent light-fields has been limited by the technology available. Existing luminance and illuminance meters, which are generally capable of sampling one sample point per orientation, pose a practical limitation on the sampling density possible around a point in a space. A method using digital cameras, which permits the rapid capture and recording of high resolution angularly sampled luminous flux, is presented. Beyond providing the information required to calculate the illuminance vector and associated vector/scalar ratio, the luminance and illuminance solids can also be determined, providing a more complete description of the light-field at a point. A method is presented to computationally calculate the illuminance solid from the spherical luminance maps. The measurement and calculation of the vector/scalar ratio using 4 or 6 sample points, as is common in the literature, is analysed in terms of their potential error compared to the ideal case. The error is shown to diminish greatly at higher sample rates. In conclusion, digital cameras can be used as efficient tools for rapidly capturing data with a high angular frequency permitting the accurate calculation of vector/scalar ratios and illuminance and luminance solids. A new descriptor for diffuseness which fully exploits the additional data made available is suggested using the standard deviation of illuminance maps. Unlike the vector/scalar ratio, the standard deviation can effectively distinguish between point source and large area light sources, which is particularly relevant in the comparison of daylight and artificially lit spaces.

Keywords: light-field, vector/scalar ratio, diffuseness, high dynamic range imaging, digital photography, daylighting

INTRODUCTION

The *light-field*, a function that describes the amount of light travelling in every direction through a point in space, has been represented in the literature [6], as the *luminance solid* and *illuminance solid*. These representations offer a complete description of the field. A reduced form, the *illuminance vector* [4, 17, 19, 21] has also been commonly employed, often applied to the calculation of a diffuseness descriptor, the *vector/scalar ratio*.

Methods for calculating Vector/Scalar ratios within the literature are inconsistent. The two principle methods described are based on either four [4, 19] or six [21, 17] sampling planes. This paper explores the accuracy of the two methods and suggests an alternative method using a higher angular frequency for sampling. This higher sample rate is achieved with the use of digital photographic technologies which permit the rapid capture of high resolution angularly sampled luminous flux. Since the appearance of low resolution video still cameras there has been continuous interest in application of photographic technology to the field of lighting research [22, 15, 16, 1, 13, 11]. This has been due to its ability to spatially sample multiple luminance points in a

scene simultaneously, generating luminance maps. The close analogy between the luminance maps and human vision has been the primary focus of such research. Complete spherical luminance maps and their application to the sampling of light-fields have not been investigated.

THE CALCULATION OF ILLUMINANCE FROM LUMINANCE MAPS

The close relationship between the light being emitted from all surfaces seen from a point, luminance, and the light incident at this point, illuminance, a fundamental component of 3D computer graphics, has not been explored in this context, reducing the usefulness of the information made available by digital cameras. This relationship is explored by Moon and Spencer [12] in their influential book 'The Photoc Field', which builds on the work of Gershun [9] on light-fields. Moon and Spencer [12] describe a method they call the solid angle method used to calculate the illuminance at a point on a surface from the luminance of surfaces viewed by that point. This method assumes light sources of constant luminance, thereby enabling the integration of the area in an orthogonal projection. It is now defined as the *cosine law*. The law states that the irradiance or

illuminance on any surface varies as a function of the cosine of the incident angle of the light source in relation to the surface normal of the illuminated surface (equation 1). This can be applied to any manifold, as the surface tends to a plane at an infinitesimal point.

$$(1) \quad E_{\Theta} = E \cos \Theta$$

Where:

E_{Θ} is the effective illuminance of an incident light source of illuminance E with an incident angle of Θ in relation to the surface normal of the surface being illuminated.

The classical radiosity model as described by Goral et al. [10] extends the cosine law to the calculation of global illumination. This is achieved via the discretisation of all the surfaces in a system. Each point is considered a point source with no area that tends to 0 enabling the simple application of the cosine law as described in equation (2). This produces a series of linear equations that can be simply resolved computationally.

$$(2) \quad H_j = \sum_{i=1}^N B_i \cos \Theta_{ij}$$

Where:

H is the illuminance the j on a surface.

B is the luminance at point i .

Θ is the incident angle of the point i in relation to the surface normal of the surface containing point j

THE IMAGINARY HEMISPHERICAL ENCLOSURE

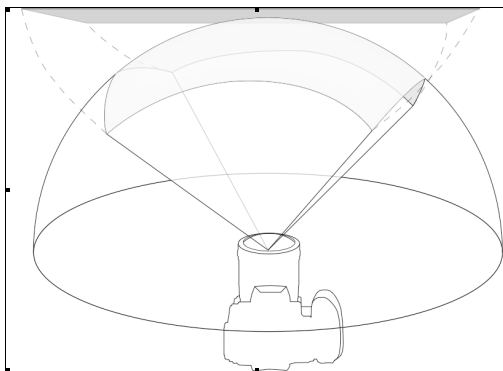


Figure 1. The camera by nature captures a fraction of a hemisphere

Generating hemispherical luminance maps, required for the calculation of illuminance via equation (2), is well suited to the camera as it is not very sensitive to depth but by nature captures images which are solid-angle fractions of a hemisphere as illustrated in Fig. 1. It is possible to construct a hemispherical luminance map with

a camera either via mosaicing of the scene as described in [2], whereby multiple images are taken while rotating the camera or with a 180° equisolid-angle fisheye lens, whereby only one image per orientation is required, producing an equisolid-angle projection of a hemisphere onto the imaging sensor as shown in Fig 2. High dynamic range bracketing (see [7] and [14]) is often required to capture the full range of luminance values found in common scenes. These techniques were first developed for use in the construction of panoramic images and VR environments as proposed in relation to Apple Inc.'s VR system [3] for the Quicktime framework.

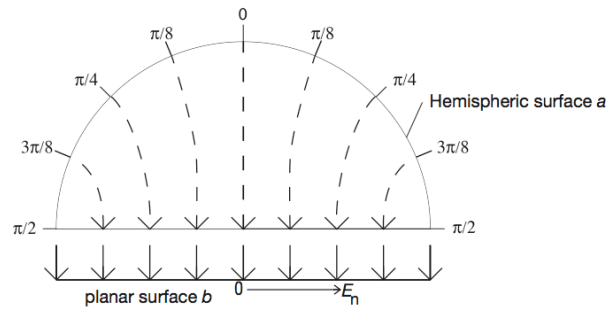


Figure 2. Equisolid-angle projection of a hemisphere onto a plane representing an imaging sensor.



Figure 3. Two luminance maps (calibrated photographs) captured with a 180° equisolid-angle fisheye lens, from the same point, facing opposite directions. (logarithmic scale)

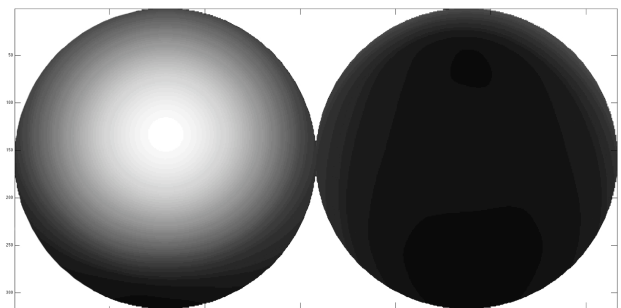


Figure 4. Illuminance map calculated from luminance map in Fig (3). Equisolid-angle projections.

Two images captured with a 180° equisolid-angle fisheye lens, from the same point, facing opposite directions, such as those in Fig (3), provide complete spherical luminance information around the point at which the camera is placed; a spherical luminance map. By employing equation (2) the illuminance at discretised points on a corresponding sphere can be calculated from the hemisphere of luminance information viewed by each respective point. Computationally this is a relatively simple procedure. The resulting illuminance map is shown in Fig (4). The illuminance maps offer an efficient visual representation of the light-field as they can be interpreted as idealised spheres with a perfectly diffusing surface. This condition is approximated by the familiar ping-pong ball.

VECTOR/SCALAR RATIO

The vector/scalar ratio is defined as the ratio between the magnitude or length of the illuminance vector and the average of the scalar illuminance values measured. It is commonly used as a relative diffuseness descriptor.

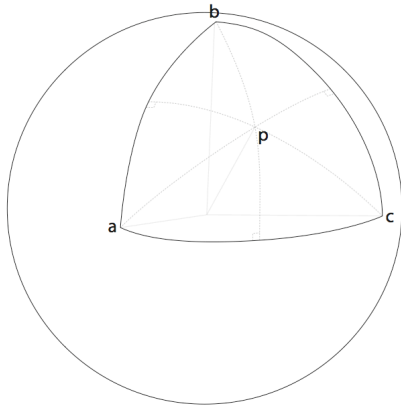


Figure 5. When a light source is locate at point *p* in relation to the sampling planes *a*, *b* and *c* the resulting summation of scalar values is at its maximum.

When calculated from a sample of six points its value for a given lighting condition is not unique as it varies according to the orientation of the sampling cube. In a worst case scenario of one point source the average scalar value, derived from only 6 values, can be shown to vary from a normalised value of 1 to $3/\sqrt{3} \approx 1.73$. The lowest value of 1 occurs when a point light source is perpendicular to one of the sampling planes *a*, *b* or *c* in Fig (5) and the highest occurs when the light source is located at *p* in relation to the sampling planes. At this point the cosine of the angle between each point *a*, *b* and *c* and *p* can be shown to be $1/\sqrt{3}$ from the dot products adding up to $3/\sqrt{3}$ times the minimum value.

This volatility, determined for 1 point source of light, still holds for 2 point sources 180° from each other. 6 evenly spaced light sources, the illuminance map of which is shown in Fig. (9), can be shown to

surpass a range of $1-\sqrt{2} \approx 1.412$ giving an error interval in excess of $\pm 20\%$.

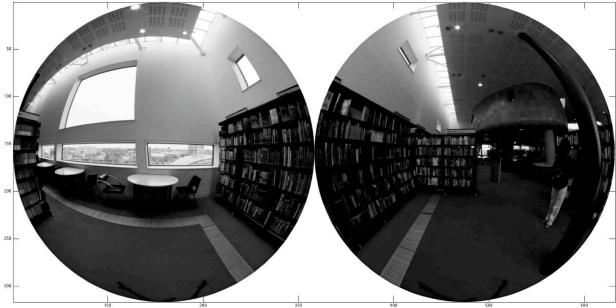


Figure 6. Luminance maps at a second point. (logarithmic scale)

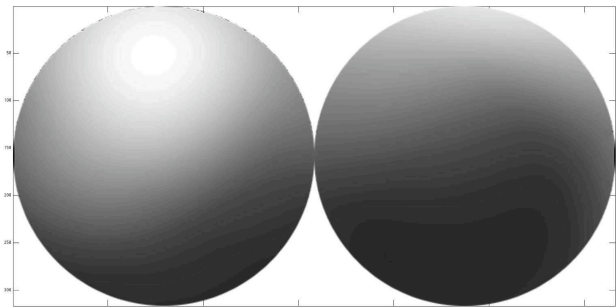


Figure 7. Illuminance map calculated from luminance maps in Fig (6). Equisolid-angle projections.

In a real-world situation, such as that in Figs. 3 & 4 the ratio of the maximum and minimum average scalar values derived from 6 equally spaced sample points is still in excess of 1:1.33 due to the prominence of one light source. It is considerably lower for the situation in Fig. (6) which has multiple light sources. The variation is only to the ratio of 1:1.08.

The illuminance vector does not suffer from the same variability as the average scalar value. Illuminance on a surface can be calculated from the summation of a finite number of equally spaced luminance points visible from the surface, each relating to a similar light cone, weighted according to the cosine law (equation 2). If the illuminance around a point is sampled with an ideal illuminance meter at 6 planes at intervals of $\pi/2$ it can be shown that the light vector can be perfectly determined.

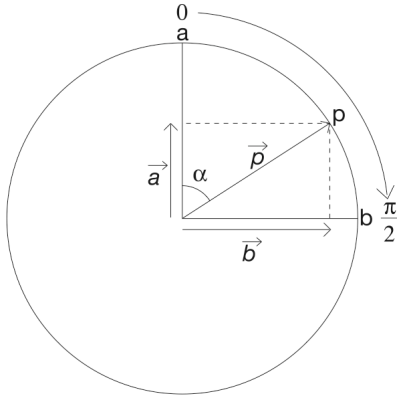


Figure 8. As the light source p rotates in relation to sample points a and b the values sampled at a and b vary according to the Cosine Law.

In figure (8) a single point source is sampled using two illuminance meters pointing in directions a and b from the centre, that is an interval of $\pi/2$. As p rotates in relation to sample points a and b the illuminance values measured at a and b vary according to the Cosine Law. Therefore:

$$(3) \quad |\vec{a}| = P \cdot \cos(\alpha)$$

and

$$(4) \quad |\vec{b}| = P \cdot \cos\left(\frac{\pi}{2} - \alpha\right) = P \cdot \sin(\alpha)$$

which perfectly describe the two vectorial components of vector \vec{P} . This ensures that both the direction and the magnitude are constant, independently of the orientation of the sample planes in relation to the point p . This extends to the 3 dimensions of a sphere, guaranteeing that the vector of every light source is represented by 3 components contained within 3 of the 6 values measured at the 6 sample planes.

Measuring the light-field with only 4 sample points is insufficient for reliably determining the illumination vector. The 4 point method which attempts to measure the horizontal along the axis with the greatest difference in illuminance is volatile and can be shown to drastically change direction while moving a short distance in a relatively uniform environment due to the absolute nature of this criteria. It is considered a poor descriptor of the light-field.

The inconsistency found in the 6 sample point method, which is purely related to the scalar component in the vector/scalar ratio, can be significantly reduced by increasing the sample rate. At several million sample points, calculated from the luminance maps captured with a digital camera, such variations, dependent on orientation, become negligible. This descriptor, however, was devised when sampling more than 6 points was practically limited. With the ability to easily

sample a scene at a significantly higher rate, it is worth re-evaluating the description of diffuseness.

STANDARD DEVIATION AS A DIFFUSENESS DESCRIPTOR

Diffuseness, as a measurement of the uniformity of the light-field at a point, is not accurately described by the Vector/Scalar ratio. The V/S ratio is unable to differentiate between evenly spaced point light sources, or real-world approximations of, and uniform large area sources. The illuminance maps in Fig. (9) are from an artificial scene with 6 evenly spaced point light sources of equal intensity. The V/S ratio using 6 sample points would yield a value approximating 0, as it would for a perfectly uniform light-field such as the conditions in an integrating sphere. These conditions are clearly distinct, both in terms of the visual experience and in terms of the way an object in the space would be illuminated yet their V/S ratios are the same.

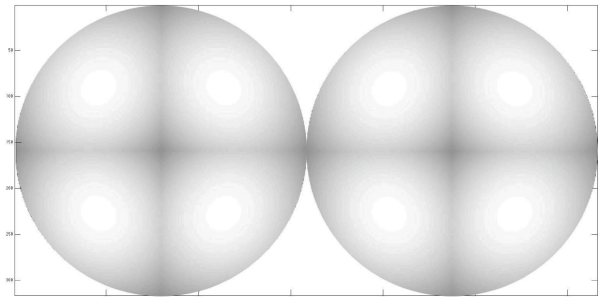


Figure 9. Illuminance map calculated from artificial luminance maps with 6 evenly spaced point light sources of equal intensity.

A true reflection of the uniformity of the light field is the standard deviation (σ) of the values around the illuminance solid. This can be calculated discretely from the illuminance maps derived from spherical luminance maps. Dividing all the illuminance values by their mean (\bar{x}) will normalise the mean to 1, making the relative σ s comparable. It can be shown that the maximum possible σ , which occurs in an environment with 1 point light source is approximately 1.301 and the theoretical minimum is 0 for a perfectly uniform light field. Dividing all σ s by 1.301 would calibrate the scale to a range of 0:1 should this be desirable for simplicity.

The lighting conditions in Fig. (3) and (4) yield a σ of 1.22, and in Fig. (6) and (7) of 0.53. The theoretical condition of Fig.(9) gives a σ of 0.10, which is clearly distinguished from a value of 0 for a perfectly uniform condition.

The standard deviation is very effective at describing uniformity and is unique for a given light-field. It

would therefore qualify as a good standard for lighting research, though it is only possible to calculate with a high sample rate.. Unlike the vector/scalar ratio, the standard deviation can effectively distinguish between point source and large area light sources, which is particularly relevant in the comparison of daylight and artificially lit spaces.

CONCLUSION

The acquisition and processing of high resolution spherical luminance information is shown to be rapid and simple with the use of an SLR digital camera and a 180° equisolid-angle fisheye lens. Existing algorithms, developed for VR engines and computer generated renderings are shown to be useful for the calculation of illuminance values from luminance maps, as long as at least one hemisphere of luminance information is captured.

The description of the illuminance vector is shown to be complete, when determined with measurements from 6 sample planes, but not from 4. The average scalar value is shown to vary according to orientation of the sampling cube when measuring 6 points, reducing its accuracy. The Vector/Scalar ratio as a diffuseness descriptor can be shown to be most accurately calculated from data sampled at a high spatial frequency such as that from the spherical luminance maps.

The effectiveness of the V/S ratio as a descriptor of diffuseness is challenged based on its inability to distinguish between point source and large area light sources, which produce different illuminance solids or maps and yet can result in the same V/S ratio. An alternative descriptor, the standard deviation of the illuminance solid, is proposed which fully exploits the additional data made available with high resolution luminance and illuminance information. The ability to distinguish between these two lighting conditions is particularly relevant in the comparison of daylight and artificially lit spaces.

REFERENCES

- [1] Bellia, L., Cesarano, F., Minichiello, F., and Sibilio, S. (2002). Setting up a ccd photometer for lighting research and design. *Building and Environment*, 37:1099–1106.
- [2] Burt, P. and Adelson, E. (1983). A multiresolution spline with application to image mosaics. *ACM Transactions on Graphics*.
- [3] Chen, S. (1995). Quicktime vr: an image-based approach to virtual environment navigation. *Proc. of the 22nd annual conference on Computer graphics and interactive technique*, pages 29–38.
- [4] CIBSE (1994). *CIBSE Code for Interior Lighting*. Chartered Institution of Building Services Engineers, London.
- [5] Cohen, M. and Greenberg, D. (1985). The hemicycle: A radiosity solution for complex environment. *Computer Graphics [Proc. SIGGRAPH '85]*, 19(3):31–40.
- [6] Cuttle, C. (1971). Lighting patterns and the flow of light. *Int. J. of Lighting Research and Technology*, 3(3):171–189.
- [7] Debevec, P. E. and Malik, J. (1997). Recovering high dynamic range radiance maps from photographs. *Proc. SIGGRAPH '97, ACM*, pages 369–378.
- [8] Doi, A. and Itoh, T. (1998). Acceleration radiosity solutions through the use of hemisphere-base formfactor calculation. *Journal of Visualization and Computer Animation*, 9(1):3–15.
- [9] Gershun, A. (1939). "the light field", moscow, 1936. translated by p. moon and g. timoshenko. *Journal of Mathematics and Physics*, XVIII:51–151.
- [10] Goral, C., Torrance, K., Greenberg, D., and Battaile, B. (1984). Modeling the interaction of light between diffuse surfaces. *Computer Graphics*, 18(2):213–222.
- [11] Inanici, M. (2006). Evaluation of high dynamic range photography as a luminance data acquisition system. *Int. J. of Lighting Research and Technology*, 38(2):123–136.
- [12] Moon, P. and Spencer, D. E. (1981). *The photic field*. Cambridge, MA, MIT Press, 1981. 265 p.
- [13] Moore, T., Graves, H., and Carter, D. J. (2000). Approximate field measurement of surface luminance using a digital camera. *Int. J. of Lighting Research and Technology*, 32(1):1–11.
- [14] Reinhard, E., Ward, G., Pattanaik, S., and Debevec, P. (2006). *High Dynamic Range Imaging: Acquisition, Display, and Image-Based Lighting*. Elsevier, Amsterdam ; London .
- [15] Rossi, G., Iacomussi, P., and Soardo, P. (1995a). The calibration of ccd matrix detectors for the measurement on photometric materials and lighting installations. *Proc. CIE 23rd Session (New Delhi)*, 1:132–133.
- [16] Rossi, G., Iacomussi, P., and Soardo, P. (1995b). A ccd multidetector for the measurement of the luminous intensity distribution of a luminaire at short distance. *Proc. CIE 23rd Session (New Delhi)*, 1:130–131.
- [17] Simons, R. H., Bean, A. R., and Bean, A. R. (2001). *Lighting Engineering: Applied Calculations*. Elsevier Science & Technology Books.
- [18] Spencer, S. N. (1992). Photorealism in Computer Graphics, chapter The hemisphere radiosity method: a tale of two algorithms, pages 127–135. Springer.
- [19] Szokolay, S., Brisbin, C., and Brisbin, C. (2004). *Introduction to Architectural Science: The Basis of Sustainable Design*. Elsevier Science, 1 edition.
- [20] Watt, A. (2000). *3D computer graphics*. Addison-Wesley, Harlow.
- [21] Wilson, J. R., Megaw, T., Corlett, N., and (author) Peter A Howarth (2005). *Evaluation of Human Work*. Taylor & Francis, Inc.
- [22] Yamaya, T. and Ohtani, Y. (1995). On a measure method of configuration factor distribution in interior by the use of an electronic still video image. *Proc. CIE 23rd Session (New Delhi)*, 1:234–235.